Combustion Reactions in Silane-Air Flames II. Counterflow Diffusion Flame

Seishiro FUKUTANI,* Nílson KUNIOSHI, Yasuhiro UODOME, and Hiroshi JINNO†
Department of Industrial Chemistry, Faculty of Engineering, Kyoto University, Yoshida-honmachi, Sakyo-ku, Kyoto 606
†Department of Chemistry, Faculty of Science and Engineering, Sophia University, Kioicho 7-1, Chiyoda-ku, Tokyo 102
(Received April 1, 1991)

A detailed chemical reaction scheme and a full set of governing equations for fluid dynamics were used to elucidate the chemical and physical phenomena involved in a silane–air counterflow diffusion flame, where the fuel and air issue from the lower and upper nozzles, respectively. It was found that a stagnation surface, where the axial velocities fall down to zero, is kept in a position slightly shifted to the upper side, dividing the system into two zones: the upper air side and the lower fuel side; after leaving the nozzle silane begins to dissociate itself into SiH_2 and H_2 when it reaches the region of rising temperature; oxygen penetrates into the fuel side by diffusion and reacts with H_2 forming OH radicals and H atoms. The produced SiH_2 is further dehydrogenated to SiO via HSiO; comparing with premixed flames, the diffusion flames have large local equivalence ratios, so that the combustion reactions in the latter flames occur through a different mechanism.

Opposite flow of gaseous fuel and air originates a stagnation point at an intermediate position between the two nozzles on the center line. The fuel and air are mixed each other within a narrow region near the stagnation point mainly due to diffusion and can hold stably a diffusion flame as shown in Fig. 1 if the flow velocities of the fuel and air do not exceed certain critical values. The flame maintained in the stagnation area is called a counterflow diffusion flame and has the simplest structure among the various types of diffusion flames.

Silane–air mixtures are very reactive and hence the gas mixtures should be treated carefully to avoid eventual explosions. In diffusion flames, on the contrary, the characteristic time of the diffusion process which mixes the fuel and air is usually longer than that of the chemical reactions, so that the former process controls the rate of the whole combustion phenomenon. Diffusion flames of silane are, therefore, preferred to premixed flames in both academic and industrial fields.

The mechanisms of chemical reactions occurring in diffusion flames, however, are not necessarily the same as those in the corresponding premixed flames. This investigation aims to elucidate the mechanism of combustion reaction of a silane–air counterflow diffusion flame and also its structure by means of computer simulation.

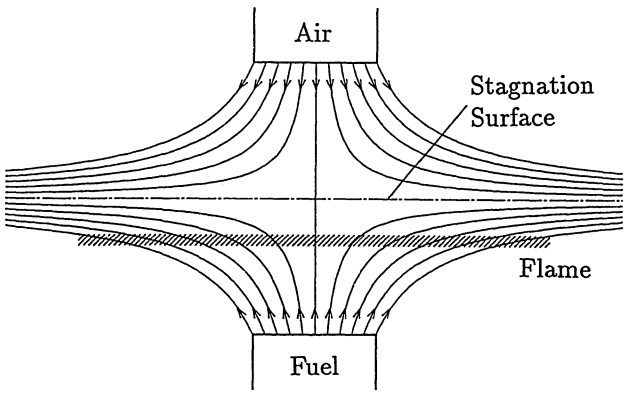

Fig. 1. Schematic figure of a counterflow diffusion flame.

Since diffusion flames have more complicated structures than premixed flames, their theoretical investigations have been predominantly based on the simple model called Burke–Schumann flame sheet model.[1] This model is constructed upon the following assumptions; (1) fuel and air react with a rate much larger than their diffusion rates so that the reaction zone is thin enough to be considered as a geometrical plane; (2) the ratio between the diffusion rates of fuel and air into the reaction zone equals the stoichiometry of the combustion reaction of both components or, in other words, the reaction zone is located at a position so that the above condition is satisfied. The Burke–Schumann model has been applied to various kinds of diffusion flames and derived many useful results.[2–6] However, most of those researches have necessarily represented their combustion reactions with overall reactions or replaced them with correspondent exothermic processes to simplify the analyzing algorithms.

The application of one-step reaction approximations is not appropriate, in particular, for diffusion flames where combustion reactions take place step by step such as methane[7] and silane flames.[8] A model containing a full reaction scheme can describe precisely the reaction mechanism and details of the flame structure such as the distributions of temperature, reaction rates and chemical species.

Theoretical studies have been done on counterflow diffusion flames by various workers;[9,10] in most of their studies the flames are treated as hypothetical one-dimensional flames by simulating only along the center line. The one-dimensional treatment of such diffusion

flames, however, is not satisfactory because the flames do not strictly possess homogeneous structures along any radial axis. Both full reaction scheme and detailed fluid mechanics are included in the model used in this investigation.

Simulation Model

The simulation model for the silane–air counterflow diffusion flame treated here was formulated under the same assumptions made in the previous work of this series[8] plus the additional condition of axial symmetry of the flame. The governing equations can be written as:

$$\frac{\partial \rho}{\partial t}+\frac{1}{r}\frac{\partial}{\partial r}(\rho u r)+\frac{\partial}{\partial z}(\rho v)=0 \tag{1}$$

$$\frac{\partial \rho u}{\partial t}+\frac{\partial \rho u^2}{\partial r}+\frac{\partial \rho uv}{\partial z}=\frac{\partial}{\partial r}\left[\mu\left\{2\frac{\partial u}{\partial r}-\frac{2}{3}\left(\frac{1}{r}\frac{\partial}{\partial r}(ur)+\frac{\partial v}{\partial z}\right)\right\}\right]+\frac{\partial}{\partial z}\left[\mu\left(\frac{\partial u}{\partial z}+\frac{\partial v}{\partial r}\right)\right]+\frac{2\mu}{r}\left(\frac{\partial u}{\partial r}-\frac{u}{r}\right)-\frac{\partial p}{\partial r} \tag{2}$$

$$\frac{\partial \rho v}{\partial t}+\frac{\partial \rho uv}{\partial r}+\frac{\partial \rho v^2}{\partial z}=\frac{\partial}{\partial z}\left[\mu\left\{2\frac{\partial v}{\partial z}-\frac{2}{3}\left(\frac{1}{r}\frac{\partial}{\partial r}(ur)+\frac{\partial v}{\partial z}\right)\right\}\right]+\frac{1}{r}\frac{\partial}{\partial r}\left[\mu r\left(\frac{\partial u}{\partial z}+\frac{\partial v}{\partial r}\right)\right]-\frac{\partial p}{\partial z}-\rho g \tag{3}$$

$$\frac{\partial c_p \rho T}{\partial t}+\frac{\partial c_p \rho Tu}{\partial r}+\frac{\partial c_p \rho Tv}{\partial z}=\frac{1}{r}\frac{\partial}{\partial r}\left(\lambda r\frac{\partial T}{\partial r}\right)+\frac{\partial}{\partial z}\left(\lambda\frac{\partial T}{\partial z}\right)+\sum_i D_i\rho\frac{\partial h_i}{\partial r}\frac{\partial \omega_i}{\partial r}+\sum_i D_i\rho\frac{\partial h_i}{\partial z}\frac{\partial \omega_i}{\partial z}-\sum_i h_i\varphi_i \tag{4}$$

$$\frac{\partial \rho\omega_i}{\partial t}+\frac{\partial \rho\omega_i u}{\partial r}+\frac{\partial \rho\omega_i v}{\partial z}=\frac{1}{r}\frac{\partial}{\partial r}\left(D_i\rho r\frac{\partial \omega_i}{\partial r}\right)+\frac{\partial}{\partial z}\left(D_i\rho\frac{\partial \omega_i}{\partial z}\right)+\varphi_i \tag{5}$$

$$p=\rho RT\sum_i\frac{\omega_i}{m_i} \tag{6}$$

where t is the time, r and z the radial and axial distances, u and v the radial and axial flow velocities; and h_i, ω_i, and φ_i are the enthalpy, the mass fraction and the production rate due to chemical reactions of the i-th species. The viscosity μ, the thermal conductivity λ and the diffusion coefficient D of the components were estimated, respectively, using Hirschfelder's, Eucken's, and Hirschfelder's approximated equations.[11] The other thermodynamic data, including the equilibrium constants were obtained from JANAF data.[12]

The partial differential equations were transformed into the corresponding finite difference equations based on the control-volume method.[13] The resulting finite difference equations were solved iteratively until time-independent solutions were obtained.

The reaction scheme used in this investigation is the same as that in the previous work, and composed of forty-five pairs of elementary reactions among SiH_4, SiH_3, SiH_2, SiH_2O, HSiO, SiO, SiO_2, OH, H, O, HO_2, H_2O_2, H_2O, H_2, O_2, and N_2. Silicon dioxide is present in the solid or liquid phase and hence the produced SiO_2 is assumed to disappear from the gaseous reaction system; therefore the steps producing SiO_2 from SiO do not have their reverse reactions. Nitrogen is assumed to be inert and any NO_x production reactions are not included in the reaction scheme.

The following conditions were imposed on the system as the boundary conditions:

1. A mixture of 5% of silane and 95% of nitrogen and air issue in the opposite directions from lower and upper nozzles, respectively, with uniform flow velocity of 0.3 m s^{-1} at 298 K. The two nozzles are 8 mm in diameter, and located oppositely with a displacement of 10 mm.
2. Nitrogen flows with constant velocity of 0.3 m s^{-1} outside both nozzles in order to stabilize the flow of the fuel and air.
3. The gradients of all dependent variables are zero at the lateral boundaries.

Results and Discussion

Flame Structure. The combustion conditions given above can provide a stable diffusion flame without any turbulence nor vortexes.

Figure 2 shows the flow velocity and temperature distributions over the whole calculation area. The points where the axial flow velocity becomes zero define the stagnation surface; on the center line, the stagnation point is located at 5.4 mm above the fuel nozzle. The axial velocity temporarily increases by about 0.05 m s^{-1} at the lower edge of the high-temperature region because of the sharp temperature rise; the momentary increase in the axial velocity observed at the edges of the high-temperature region is characteristic of this type of diffusion flames.[10] The radial component of the flow velocity increases as the gas flows away from the nozzles and becomes 0.61 m s^{-1} at the lateral boundary.

The high-temperature region is confined into a fairly narrow zone of about 2 mm wide and is unevenly distributed to the side lower than the stagnation surface.

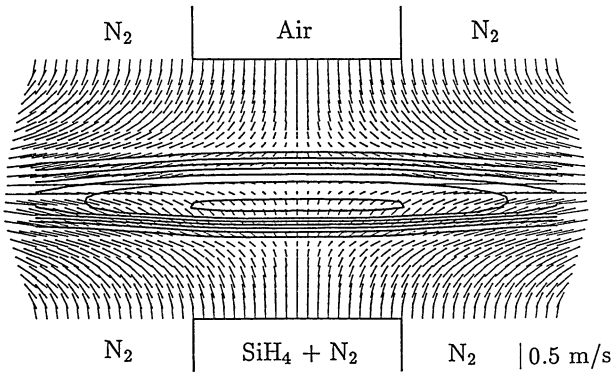

Fig. 2. Distributions of the flow velocity and temperature. The two nozzles are 8 mm in diameter and separated by a distance of 10 mm. The contour lines of the temperature are drawn for every 250 K from 500 K to 2000 K.

The temperature reaches about 2000 K, which is the highest temperature in this flame, at 4.0 mm in height on the center line; the maximum value is much lower than that found in premixed flames[8] due to the excess dilution of the combustion gas with nitrogen. The averaged temperature gradient in the axial direction is about 1420 K mm^{-1} at the lower side and larger than that at the upper side suggesting that exothermic reactions occur intensely at the lower side. The radial gradients of the temperature are almost zero within the cylindrical region between the nozzles.

The concentrations of the reactants and products are shown with contour lines in Fig. 3. As described above silicon dioxide is assumed to exist in the condensed states and is removed out from the gaseous reaction system. Its amount should be expressed with the number and the size of deposited silicon dioxide particles but it is expressed here, for convenience' sake, with the mole fraction defined as the molar concentration over the total molar concentration of the gaseous components.

The fuel and oxygen are both exhausted at about 4 mm in height. The following two points should be noted on their profiles; (1) oxygen penetrates deeply into the lower side across the stagnation surface; (2) a gap of about 0.2 mm wide is observed between the disappearing positions of the fuel and oxygen even on the center line and such a displacement is much wider than the reaction zone of silane–air premixed flames.[8]

The location and thickness of the fuel-and-air mixing region depend on the chemical and transport properties of the gases such as reactivity and diffusivity. The binary diffusion coefficient between oxygen and nitrogen is about 1.6×10^{-4} $m^2 s^{-1}$ at 1000 K, for instance, and about 1.6 times as large as that between silane and nitrogen. The diffusional flux of oxygen overwhelms that of silane and this species penetrates into the lower side transgressing the stagnation surface. In a hydrogen–air counterflow diffusion flame, on the contrary, hydrogen enters deeply into the air side over the stagnation surface.[10] Hereafter the regions below and above the stagnation surface will be called fuel side and air side, respectively.

As for the second point, the empty region of both fuel and air indicates that the Burke–Schumann assumption of the diffusion-rate ratio equal to the stoichiometry of reaction between the two components is not valid in this flame and that the fuel and oxygen do not directly react each other.

Silicon dioxide is present in a narrow region lying between the stagnation surface and the fuel-and-oxidizer exhaustion layer; the confinement suggests that the SiO_2 formation occurs just below the stagnation surface and, in addition, the species is carried by the upstream flow toward the stagnation surface. The other final product, water, however, extends widely due to its movability.

Figure 4 shows the distributions of silicon-containing intermediate species having important roles. The rest three species are present in small amounts. The maximum mole fractions are 2.9×10^{-3} for SiH_3, 6.9×10^{-4} for SiH_2O, and 2.1×10^{-5} for HSiO; the amounts of the last two species, in particular, are more than 100 times as small as those in the premixed flame. The presence of this group of species is concentrated in the fuel side, while SiH_2O and HSiO are distributed in regions with radius larger than 6 mm.

The hydrogen–oxygen-containing species, however, extend over fairly wide regions even in the air side crossing over the stagnation surface as shown in Fig. 5. Hydroperoxyl radicals distribute mainly in the region above the stagnation surface though the amount is much smaller than the three active species OH, H, and O.

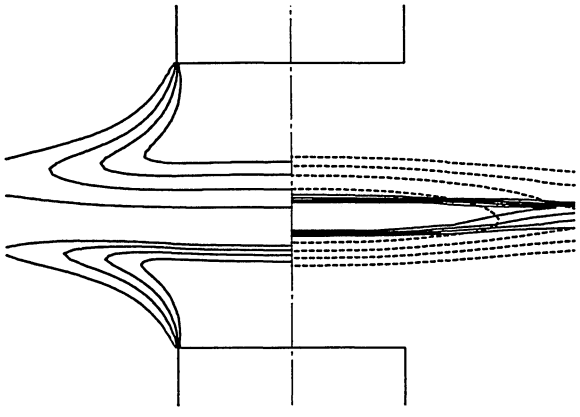

Fig. 3. Distributions of the stable species mole fractions. The contour lines for each species correspond to four values of equal intervals from the minimum to the maximum mole fraction (x_{max}). The mole fractions of SiH_4 ($x_{max}=5.0\times10^{-2}$) and O_2 ($x_{max}=2.1\times10^{-1}$) are shown in the left half of the figure, and those of SiO_2 ($x_{max}=1.3\times10^{-1}$) and H_2O ($x_{max}=4.5\times10^{-2}$) are shown in the right half with the solid and the dashed lines, respectively.

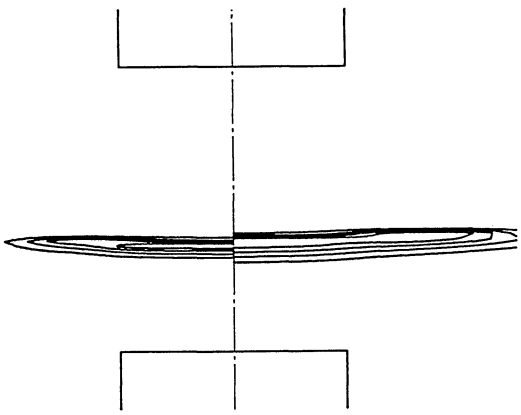

Fig. 4. Distributions of the mole fractions of silicon-containing intermediate species. The four contour lines are defined as those in Fig. 3. The mole fraction of SiH_2 ($x_{max}=8.9\times10^{-3}$) is shown in the left half and that of SiO ($x_{max}=4.1\times10^{-3}$) in the right half.

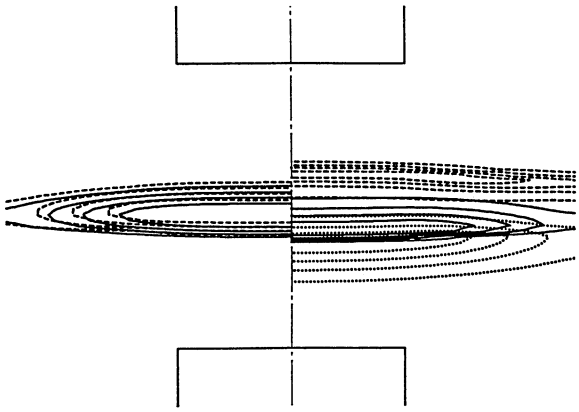

Fig. 5. Distributions of the mole fractions of hydrogen–oxygen-containing intermediate species. The four contour lines are defined as those in Fig. 3. The mole fractions of OH ($x_{max}=3.4\times10^{-3}$) and O ($x_{max}=1.9\times10^{-3}$) are shown with the solid and dashed lines, respectively, in the left half and those of H_2 ($x_{max}=8.3\times10^{-3}$), H ($x_{max}=1.9\times10^{-3}$), and HO_2 ($x_{max}=2.0\times10^{-5}$) are shown with the dotted, solid and dashed lines, respectively, in the right half of the figure.

According to Figs. 4 and 5 the silicon-containing and hydrogen–oxygen-containing species are present in two regions clearly divided at about 4 mm in height, which just coincides with the exhaustion zone of the fuel and air suggesting that the reactions of silicon-containing species and those of hydrogen–oxygen-containing species take place separately in the fuel and the air sides, respectively.

Combustion Reaction. Figure 6 shows the distributions of the predominant reactions occurring at the early silane combustion and the species participating in that step. Silane is dehydrogenated by hydrogen atoms at a height as low as 3.5 mm through reaction

$$SiH_4 + H \longrightarrow SiH_3 + H_2, \qquad (R25)$$

and the produced SiH_3 further reacts also with hydrogen atoms through reaction

$$SiH_3 + H \longrightarrow SiH_2 + H_2. \qquad (R28)$$

About 35% of SiH_4 is transformed into SiH_2 by the above pair of reactions even at very low positions of the fuel side, where the temperature is about 1400 K. The rest of the fuel is directly decomposed to SiH_2 by reaction

$$SiH_4 \rightarrow SiH_2 + H_2 \qquad (R22)$$

in a region located 0.2 mm above that for reactions (R25) and (R28). It is noticeable that the reactions converting SiH_4 to SiH_2 do not require O_2 or any oxygen-containing species.

Figure 7 shows the distributions of the other silicon-containing species and the reactions yielding the products up to SiO_2. The SiH_2 formed by either of the above reaction pathways is oxidized through

$$SiH_2 + O_2 \longrightarrow HSiO + OH. \qquad (R32)$$

Then, the produced HSiO is immediately dehydrogenated by reactions

$$HSiO + H \longrightarrow SiO + H_2 \qquad (R39)$$

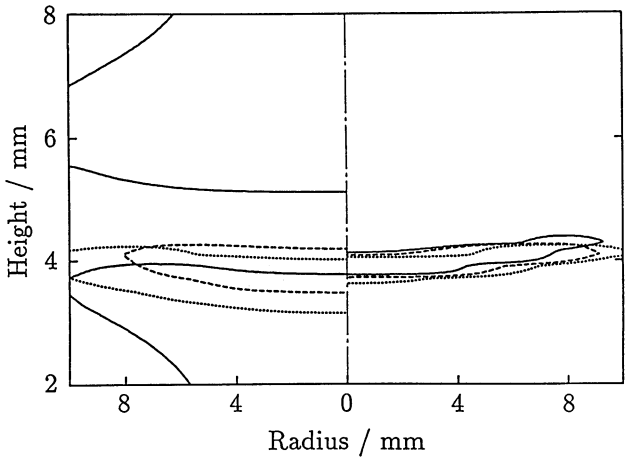

Fig. 6. In the left-hand side: distributions of SiH_4 (lower solid contour line for the mole fraction of $x=9.0\times10^{-3}$), SiH_3 (dotted line, $x=5.9\times10^{-4}$), SiH_2 (dashed line, $x=1.8\times10^{-3}$), and O_2 (upper solid line, $x=3.9\times10^{-2}$); in the right-hand side: distributions of reactions (R22) (solid contour line for the reaction rate of $\varphi=57$ mol m^{-3} s^{-1}), (R25) (dotted line, $\varphi=43$ mol m^{-3} s^{-1}), and (R28) (dashed line, $\varphi=33$ mol m^{-3} s^{-1}). The reaction numbers correspond to those in the text. The mole fractions and the reaction rates designated by the contour lines are 80% of the corresponding maximum values.

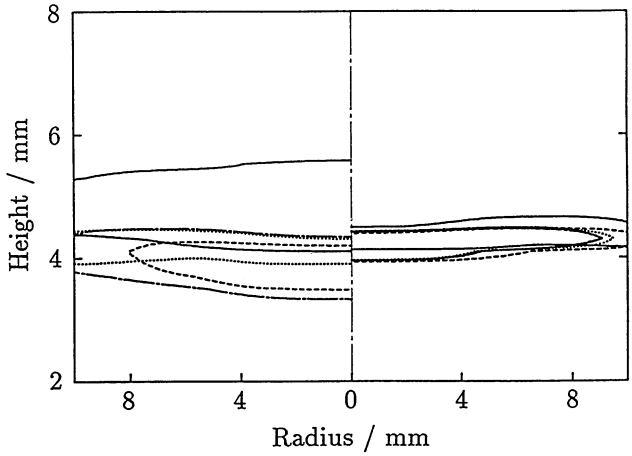

Fig. 7. In the left-hand side: distributions of SiH_2 (dashed line, $x=1.8\times10^{-3}$), HSiO (dotted line, $x=4.3\times10^{-6}$), SiO (dotted-dashed line, $x=8.2\times10^{-4}$), and SiO_2 (solid line, $x=2.7\times10^{-2}$); in the right-hand side: distributions of reactions (R32) (dotted line, $\varphi=66$ mol m^{-3} s^{-1}), (R38) and (R44) (the two dotted-dashed lines, for $\varphi=23$ mol m^{-3} s^{-1} and $\varphi=29$ mol m^{-3} s^{-1}, respectively, lie upon each other), (R39) (dashed line, $\varphi=34$ mol m^{-3} s^{-1}), and (R45) (solid line, $\varphi=39$ mol m^{-3} s^{-1}).

or

$$HSiO + M \longrightarrow SiO + H + M. \quad (R38)$$

According to Fig .7 the SiO-producing reactions are intensely activated from about 4 mm in height but the produced SiO appears even at 3 mm on the center line. The conservation equation of chemical species requires, in the steady state, that each species must keep the balance among the five terms of Eq. 5, that is, axial and radial convection and diffusion, and reaction terms; only one steady state should be realized due to given boundary conditions but independently of initial conditions. Silicon monoxide in the mesh located at 3 mm in height and on the center line, for instance, increases with a rate of 1.9×10^{-1} mol m^{-3} s^{-1} by diffusion in the axial direction, decreases with a rate of 1.6×10^{-1} mol m^{-3} s^{-1} by axial convection and is compensated with the other three terms. The reaction term is negligible as described above, and the two radial terms, particularly radial diffusion, are also small.

The final oxidation predominantly consists of reactions

$$SiO + OH \longrightarrow SiO_2 + H \quad (R44)$$

and

$$SiO + O_2 \longrightarrow SiO_2 + O. \quad (R45)$$

The former reaction occurs in lower positions.

Consequently SiH_4 is oxidized step by step according to the sequence $SiH_4 \rightarrow SiH_2 \rightarrow HSiO \rightarrow SiO \rightarrow SiO_2$; the first step is composed of two routes, the direct dehydrogenation and the route via SiH_3.

The hydrogen–oxygen-containing species required by the above reactions as reactants are hydrogen atoms at the early stages, hydroxyl radicals at the final stage and oxygen at the middle and final stages. Those species and the main reactions related to them are shown in Fig. 8. The comparison of Figs. 7 and 8 indicates that the reactions among the hydrogen–oxygen-containing species take place at higher positions than those occurring among the silicon-containing species.

Hydrogen liberated by reaction (R22) reacts with oxygen at positions higher than 4 mm by reactions

$$O + H_2 \longrightarrow OH + H \quad (R3)$$

and

$$H + O_2 \longrightarrow OH + O. \quad (R2)$$

These are the predominant chain-branching reactions which are of great importance in almost all flames of hydrogen-containing fuel, and produce hydroxyl radicals with exponentially increasing rate. The hydroxyl radicals oxidize hydrogen to water and further produce hydrogen atoms by reaction

$$OH + H_2 \longrightarrow H + H_2O. \quad (R5)$$

Reactions (R2) and

$$OH + OH \longrightarrow O + H_2O \quad (R4)$$

proceed backward between 4 and 4.5 mm in height.

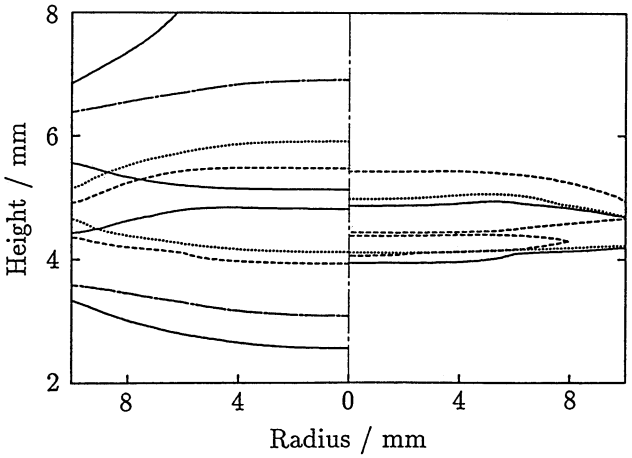

Fig. 8. In the left-hand side: distributions of H_2 (lower solid line, $x=1.7\times10^{-3}$), H (dashed line, $x=3.8\times10^{-4}$), OH (dotted line, $x=6.2\times10^{-4}$), H_2O (dotted-dashed line, $x=8.9\times10^{-3}$), and O_2 (upper solid line, $x=3.9\times10^{-2}$); in the right-hand side: distributions of reactions (R2) (upper dashed line, $\varphi=66$ mol m^{-3} s^{-1} for forward reaction and lower dashed line, $\varphi=18$ mol m^{-3} s^{-1} for backward reaction), (R3) (dotted line, $\varphi=18$ mol m^{-3} s^{-1}), and (R5) (solid line, $\varphi=39$ mol m^{-3} s^{-1}).

Oxygen and hydroxyl radicals are produced so that their insufficient supply to the lower region is compensated by those reactions. Hydrogen atoms are produced at heights above 4 mm and diffuse toward lower positions because of their large diffusion coefficient and are consumed by reactions (R25) and (R28).

In the previous paper on the combustion mechanism of silane–air premixed flames[8] two different pathways between SiH_4 and HSiO have been reported under a wide range of equivalence ratios: $SiH_4 \rightarrow SiH_3 \rightarrow SiH_2O \rightarrow HSiO$, which proceeds in low-temperature regions, and $SiH_4 \rightarrow SiH_2 \rightarrow HSiO$, occurring at high temperatures. These two routes can be clearly distinguished by the parameters of temperature and equivalence ratio. Hydroxyl radicals are the most important oxidizer in those pathways and in the former mechanism, in particular, they promote the dehydrogenation

$$SiH_4 + OH \longrightarrow SiH_3 + H_2O \quad (R27)$$

and

$$SiH_3 + O_2 \longrightarrow SiH_2O + OH \quad (R31)$$

with the cooperation of oxygen. The direct dehydrogenation of SiH_4 to SiH_2 by reaction (R22) is not accelerated until about 2000 K.

The two dehydrogenation pathways of SiH_4 are also observed in the counterflow diffusion flame; however, the one via SiH_3 does not proceed toward SiH_2O and, in addition, the reaction partners of SiH_4 and SiH_3 are hydrogen atoms instead of hydroxyl radicals. The main reason for those differences is that the local equivalence ratio in the region where the silicon-containing

species reactions occur is remarkably small in the diffusion flame so that SiH_3 is not oxidized into SiH_2O.

Conclusions

A silane–air counterflow diffusion flame was simulated using a detailed reaction scheme and complete fluid-dynamic governing equations, and the following conclusions were obtained:

(1) Oxygen which issues from the upper nozzle transgresses the stagnation surface, and hence reaction zone is formed in the fuel side. The temperature becomes maximum near the fuel-side edge of the reaction zone. Silane is preferentially oxidized in the fuel side of the reaction zone, and then the liberated hydrogen is oxidized producing active species necessary for silane combustion such as hydroxyl radicals and hydrogen atoms.

(2) Silane reacts through the sequence: $SiH_4 \rightarrow SiH_2 \rightarrow HSiO \rightarrow SiO \rightarrow SiO_2$. The first step is composed of two alternative routes: the direct dehydrogenation of SiH_4 to SiH_2 and the route $SiH_4 \rightarrow SiH_3 \rightarrow SiH_2$; the direct hydrogenation is predominant though the activation energy of unimolecular dissociation (R22) is much larger than the initiation reaction of the indirect dehydrogenation. In the premixed flames a large variety of species are present even at early stages of the reactions, but in the diffusion flame the initiation reaction, in particular, inevitably proceed in the state of insufficient oxygen-containing species relatively to premixed flames. The fuel oxidation up to silicon dioxide, therefore, occurs only in small amounts in the fuel side.

References

1) S. P. Burke and T. E. W. Schumann, *Ind. Eng. Chem.*, **20**, 998 (1928).
2) F. G. Roper, *Combust. Flame,* **29**, 219 (1977).
3) R. E. Mitchell, A. F. Sarofim, and L. A. Clomburg, *Combust. Flame,* **37**, 227 (1980).
4) R. A. Allison and J. F. Clarke, *Combust. Sci. Tech.*, **23**, 113 (1980).
5) R. A. Allison and J. F. Clarke, *Combust. Sci. Tech.*, **25**, 97 (1981).
6) M. Klajn and A. K. Oppenheim, "Nineteenth Symposium (International) on Combustion," The Combustion Institute, Pittsburgh (1982), p. 223.
7) S. Fukutani, K. Sakaguchi, N. Kunioshi, and H. Jinno, *Bull. Chem. Soc. Jpn.*, **64**, 1623 (1991).
8) S. Fukutani, Y. Uodome, N. Kunioshi, and H. Jinno, *Bull. Chem. Soc. Jpn.*, **64**, 2328 (1991).
9) G. Dixon-Lewis, T. David, P. H. Gaskell, S. Fukutani, H. Jinno, J. A. Miller, R. J. Kee, M. D. Smooke, N. Peters, E. Effelsberg, J. Warnatz, and F. Behrendt, "Twentieth Symposium (International) on Combustion," The Combustion Institute, Pittsburgh (1984), p. 1893.
10) S. Fukutani, *Nenshokenkyu,* **75**, 1 (1987).
11) R. H. Perry and C. H. Chilton, "Chemical Engineer's Handbook," 5th ed, McGraw-Hill, New York (1973).
12) M. W. Chase, Jr., C. A. Davies, J. R. Downey, Jr., D. J. Frurip, R. A. McDonald, and A. N. Syverud, "JANAF Thermochemical Tables," Part I and II, 3rd ed, The American Chemical Society and the American Institute of Physics (1985).
13) S. V. Patankar, "Numerical Heat Transfer and Fluid Flow," Hemisphere Publishing Co., New York (1980), Chap. 3.